Chunlin Chen*, Ling Zhang and Jean Lehmann

Thermodynamic Modelling of Phosphorus in Steelmaking Slags

Abstract: The published phase diagrams of some key P_2O_5-containing systems which are relevant to the steelmaking slag and the available experimental data on phosphorus partitioning between liquid iron and slags consisting of SiO_2-Al_2O_3-Fe_2O_3-FeO-MnO-MgO-CaO-Na_2O have been reviewed and assessed. A set of data under carefully controlled experimental conditions, which was considered to be more reliable based on the assessment, was selected for optimising the generalised central atom (GCA) model parameters of phosphorus-containing slag systems. The developed model database is proved to be able to represent the liquidus temperature of some key P_2O_5-containing systems and the phosphorus distribution ratio between the steelmaking slags and liquid iron reasonably well. With the developed GCA model database, the dephosphorization reaction in the steelmaking process was modelled under various operating conditions such as slag chemistry and temperature. The results show that the phosphorus distribution ratio between the slags and liquid iron displays a maximum point with variation of the FeOx content in the slag. It also shows that the phosphorus deportment to the slag is favored by decreasing the operating temperature and MgO content, and increasing the CaO/SiO_2 ratio in the slag. Comparison with the model of the phosphorus distribution data from a commercial BOS furnace shows that operating conditions do not permit to reach P equilibrium contents. The dis-equilibrium degree of P was found to be increased with increasing slag viscosities.

Keywords: phosphorus, steelmaking slag, thermodynamic modeling, GCA model, dephosphorization

PACS® (2010). 05.70.Ce

***Corresponding author: Chunlin Chen:** CSIRO Process Science and Engineering, Clayton, Victoria, Australia
E-mail: chunlin.chen@csiro.au
Ling Zhang: CSIRO Process Science and Engineering, Clayton, Victoria, Australia
Jean Lehmann: ArcelorMittal Global R&D, Maizières-lès-Metz, France

1 Introduction

The desire to reduce the impurity content of steels as much as possible has been the driving force for a large number of investigations into the thermodynamics and kinetics of the metal/slag/gas reactions which occur in the basic oxygen steelmaking processes. The importance of the dephosphorisation reaction has been identified since the early development of the basic steelmaking processes, and the interest in the thermodynamics of this reaction has been growing over the last four decades. Numerous investigations have been carried out with the aim of determining the equilibrium distribution of phosphorus between slag and metal for basic slags with various compositions. Based on the published data, the correlations for the phosphorus distribution between the metal and slag have been derived in terms of slag composition and the temperature of the metal/slag interface. However, to date not one of the published correlations is universally accepted and valid in all slag systems. Furthermore, the discrepancies between the correlations derived from different published data are sometimes large enough to result in contradictory conclusions regarding the approach to equilibrium in steelmaking processes.

The thermodynamic properties of slag have critical process implications for many metal production processes, such as the production of clean steels, and the interaction of the alloy phase with solid or liquid oxides (non-metallic inclusions for instance). Understanding of the metal-slag interaction such as dephosphorization reaction can be greatly aided by well developed liquid oxide or slag models. The Cell model [1] developed at ArcelorMittal Global R&D Maizières Process (formerly IRSID) during the 80's was the first comprehensive thermodynamic model for metallurgical slags. This slag model has been further extended to include second and third anions, i.e., S^{2-}, F^- [2], and other common oxide species, such as P_2O_5, Cr_2O_3 [2] and TiO_2 [3] in steel making slags. The CSIRO group adopted and further developed the cell model beyond the iron and steel application. The models and the database include a substantial list of oxide species commonly found in both ferrous and non-ferrous metal smelting. The model was incorporated in a computational

package, Multi-Phase Equilibrium (MPE) software [4, 5]. Models of transport properties of the slag are also incorporated. The MPE software has been used by researchers and plant metallurgists for the prediction of the multiphase equilibria, and the viscosity and electrical conductivity of the slags.

A more recent development in this domain, conducted jointly by ArcelorMittal Global R&D Maizières Process and CSIRO Process Science and Engineering, is the Generalized Central Atom model [6]. This model is a generalization of the Central Atom model proposed in the 1970's by Lupis and co-workers [7] for modelling solid steel, which has now been extended to cover molten oxides and alloys. Recent work has shown how this model could greatly improve the performances of the Cell model for slags and how promising its application to liquid steel is, especially for high alloyed grades or segregated solutions [6, 8]. In this study, the published phase diagrams of some key P_2O_5-containing systems which are relevant to the steelmaking slag and the available experimental data on phosphorus partitioning between liquid iron and slags consisting of SiO_2-Al_2O_3-Fe_2O_3-FeO-MnO-MgO-CaO-Na_2O have been reviewed and assessed. A selected set of data was used for optimising the GCA model parameters of phosphorus-containing slag systems. With the developed GCA model database, the dephosphorization reaction in the steelmaking process under various operating conditions such as slag chemistry and temperature was modelled. The plant data on the P partitioning between metal and slag was also analyzed by using the model.

2 GCA model

In the GCA model the structure of liquids is described in terms of cells composed of a central atom and its shell of nearest neighbours. In a system with m components (elements), t cations and (m-t) anions, the cell will be denoted as

$i_1, i_2, \ldots i_k, \ldots i_t$	Atoms on cationic shell
J	Central atom
$j_{t+1}, \ldots j_r, \ldots j_m$	Atoms on anionic shell

In such a cell, around the central atom **J,** either a cation or an anion, there are i_1 cations #1, i_2 cations #2... on the cation shell and j_{t+1} anions #t+1, j_{t+2} anions of #t+2... on the anion shell. Similar to the cell model, there are two kinds of parameters in the GCA model, namely the formation and the interaction energy. The formation of the cell is $\varphi^J_{\{i\},\{j\}}$ where J represents the central atom and {i} and {j} presents the whole set of cations and anions respectively. For the sake of simplicity, this energy term is assumed to be the sum of the contributions of the two shells:

$$\varphi^J_{\{i\},\{j\}} = \varphi^J_{\{i\}} + \varphi^J_{\{j\}} \tag{1}$$

To reduce the number of parameters, different assumptions can be formulated to describe the energy variation for the central atom according to the composition of the chemical neighbourhood. To be compatible with the expression of the cell model [1] the following form was chosen for the GCA model:

$$\varphi^J_{\{i\}} = \sum_{k=1}^{t} i_k \varphi^J_{kk} + \frac{1}{2} \sum_{\substack{k,l=1 \\ k \neq l}}^{t} i_k i_l \varphi^J_{kl} \tag{2}$$

The k and l in equation refer to the elements on cation shell. Equation (2) applies to both cations and anions. For the metallurgical slags, the parameters φ^J_{kl} are inherited from the cell model where they are associated with the formation of an "asymmetric" cell from the two corresponding symmetric ones:

$$\frac{1}{2}\text{K-J-K} + \frac{1}{2}\text{I-J-I} \rightarrow \text{K-J-I} \tag{3}$$

Beside these formation energy parameters, interaction energy terms have been considered still to stay compatible with the cell model. The contribution of these terms to the Gibbs free energy has the following expression:

$$E = \frac{1}{2} RT \{ \sum_{j=1}^{m} \sum_{\{i\},\{j\}} N_j p^J_{\{i\}\{j\}} \ln Q^J_{\{i\}\{j\}} \} \tag{4}$$

where N_J is the number of atoms J and $p^J_{\{i\}\{j\}}$ the probability to have the configuration {i}{j} around the atom J.

Some simple assumptions were introduced for these interactions. First, as for formation energy parameters, an additive rule has been taken:

$$\ln Q^J_{\{i\}\{j\}} = \ln Q^J_{\{i\}} + \ln Q^J_{\{j\}} \tag{5}$$

Then, this interaction was assumed to vanish if all the atoms situated on this shell are not of the same nature:

$$\ln Q^J_{\{i\}} = \ln Q^J_K \neq 0 \; \textit{if and only if} \; i_k = Z_j \tag{6}$$

Finally, the following expression was adopted for $\ln Q_k^J$:

$$RT \ln Q_k^J = \frac{1}{2N_R}\{\sum_{i=1}^{t} Z_i N_i E_{ki}^J + \sum_{j=t+1}^{m+1} Z_j N_j E_{jk}^J\} \quad for\ J > t \quad (7)$$

$$RT \ln Q_l^J = \frac{1}{2N_S}\{\sum_{j+t+1}^{m+1} Z_j N_j E_{lj}^J + \sum_{k=1}^{t} Z_k N_k E_{kl}^J\} \quad for\ J \le t \quad (8)$$

N_R and N_S are the number of cations and anions respectively.

To be compatible with the cell model, the formation energy φ_{kl}^J and interaction energy E_{kl}^J were described to have a linear variation with the composition:

$$\varphi_{kl}^J = {}^0\varphi_{kl}^J + {}^1\varphi_{kl}^J \cdot x_k \quad (9)$$

$$E_{kl}^J = {}^0E_{kl}^J + {}^1E_{kl}^J \cdot x_k \quad (10)$$

where x_k is the mole fraction of element k.

Derivation of Gibbs free energy and of the chemical-potentials is described in details elsewhere by Lehmann [6]. During the database development, formation energy parameters ${}^0\varphi_{kl}^J$, ${}^1\varphi_{kl}^J$ and interaction energy parameters ${}^0E_{kl}^J$, ${}^1E_{kl}^J$ are optimized against the thermodynamic data such as the phase diagram and activity data of the target system.

3 Modelling of the phase diagrams

3.1 CaO-P_2O_5 system

It is well known that the CaO is a very effective flux agent for dephosphorization of liquid iron due to the strong interaction and formation of stable compounds between the CaO and P_2O_5. The Gibbs energy data of solid, liquid P_2O_5 and the CaO-P_2O_5 compounds in SGTE database [9] are used in the present study. The CaO-P_2O_5 model parameters listed in Table 1 were optimized against the published phase diagram data of the CaO-P_2O_5 system [10].

The comparison of the calculated phase diagram with the experimental measurements is shown in Figure 1. It can be seen that the overall fit by the model is reasonably good, particularly the stability of the compounds 2CaO.P_2O_5 and 3CaO.P_2O_5. Accurate description of the stability of 3CaO.P_2O_5 and the eutectic point between 4CaO.P_2O_5 and 3CaO.P_2O_5 is important since it is more relevant to the steelmaking process. It also has significant impact on the accuracy of the liquidus where 4CaO.P_2O_5 and 3CaO.P_2O_5 are the primary solid phases in the CaO-FeOn-P_2O_5 ternary and higher order systems.

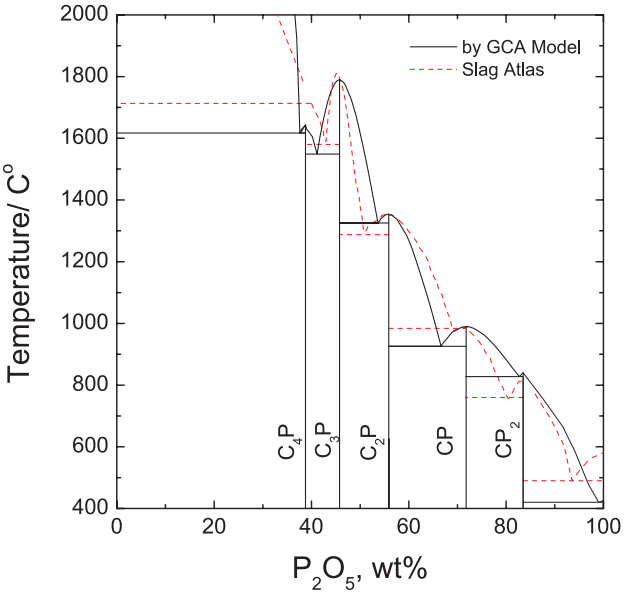

Fig. 1: Comparison between the calculated liquidus by the GCA model and the published data [10] in the CaO-P_2O_5 system.

Table 1: Slag model parameters for the CaO-FeOn-P_2O_5 system (J/mol)

CaO-P_2O_5	${}^0\varphi_{CaP}^O = -7981.25$; ${}^1\varphi_{CaP}^O = -17240$; ${}^0E_{CaP}^O = 35275$; ${}^1E_{CaP}^O = -47082$
FeO-P_2O_5	${}^0\varphi_{Fe2P}^O = -4739$; ${}^1\varphi_{Fe2P}^O = 16040$; ${}^0E_{Fe2P}^O = -4134$; ${}^1E_{Fe2P}^O = -46404$
Fe_2O_3-P_2O_5	${}^0\varphi_{Fe3P}^O = -2167$
CaO-FeOn-P_2O_5	${}^0\varphi_{Fe2P}^{Ca} = -3525$; ${}^0\varphi_{CaP}^{Fe2} = -3208$; ${}^0\varphi_{CaP}^{Fe3} = -2300$

3.2 CaO-FeOn-P_2O_5 system

The liquidus of the FeO enriched area of the FeOn-CaO-P_2O_5 system saturated with iron and under a gas mixture consisting of CO_2 and H_2 with CO_2/H_2 ratio of 9 were measured by Tromel et al. [11, 12], respectively. As shown in Figure 2, the P_2O_5 solubility in the FeO-CaO melt is less than 7 wt% at 1500°C. It can be seen that the P_2O_5 solubility increases with increasing CaO content, which suggests that CaO-P_2O_5 interaction is stronger than that of FeO-P_2O_5. The FeO-P_2O_5 and Fe_2O_3-P_2O_5 binary parameters and CaO-FeOn-P_2O_5 ternary parameters, listed in Table 1, were optimized against the published liquidus by Trömel et al. [11, 12]. The calculated Fe saturated liquidus at 1500°C, and the liquidus at 1600°C in air are shown in Figure 2a and 2b along with the experimental measurements. It can be seen that the overall fits to the liquidus at low P_2O_5 region are satisfactory.

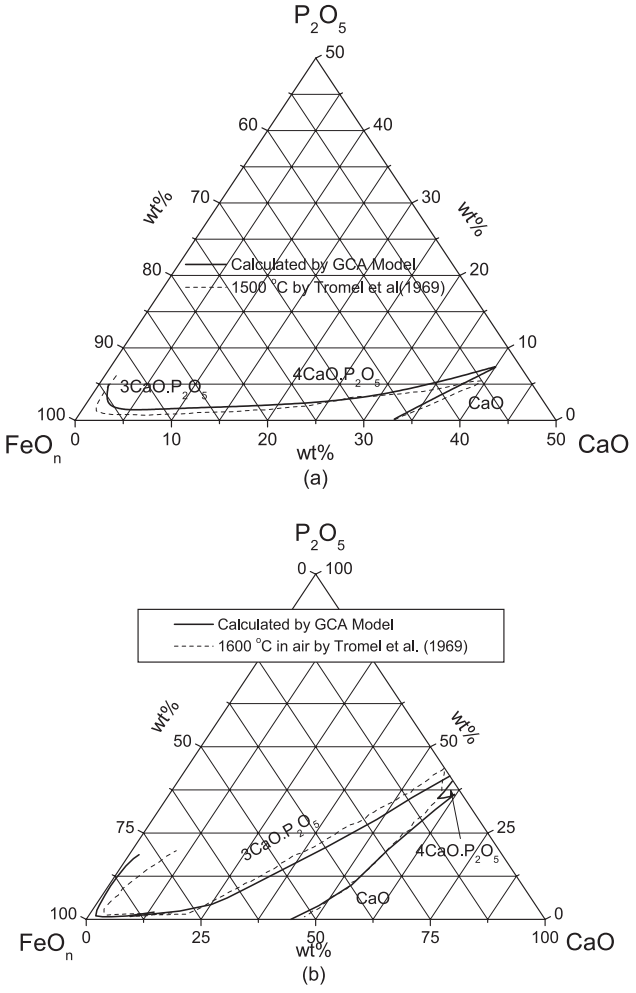

Fig. 2: Comparison between the calculated Fe saturated liquidus at 1500°C (a) and liquidus at 1600°C in air (b) by the GCA model and the experimental data [11, 12] in the Fe saturated CaO-P_2O_5-FeOn system.

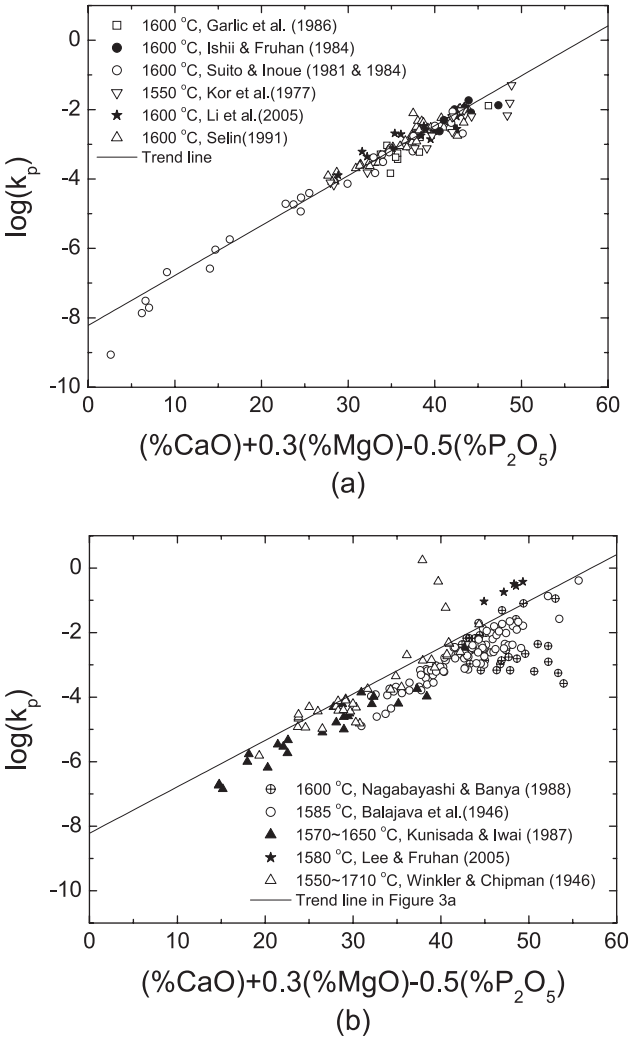

Fig. 3: Comparison of the literature data on the relationship between $\log(k_p)$ and slag chemistry [13–21, 22–24, 27, 33, 34].

4 Modelling of the P distribution between slag and metal

The dephosphorization reaction is a classical topic of steelmaking chemistry and over the years numerous investigations have been carried out with the aim of determining the equilibrium distribution of phosphorus between metal and basic slags with various compositions [13–36].

Considering that the P concentration in metal of majority data [13–36] is less than 0.1 wt%, the activity of P can be set to its concentration, when the standard state is chosen to be 1 wt% of P in metal. During the modelling, the slag composition was set to be identical to the experimental data, the model parameters were optimized by fitting the P activity in slag, which is equal to the P activity or P concentration in metal, since the slag is in equilibrium with the metal. Attempts have been made to fit the P activities in slag with both high and low concentration of P_2O_5 with GCA model. Preliminary results show that agreement between the model calculation and the experimental data is not satisfactory. Considering that the scope of the present study is the steekmaking slag with low P_2O_5 concentration (<5 wt%), the experimental data of slag with low P_2O_5 was used to optimize the model parameters.

The experimental conditions and slag chemistry covered in the studies [13–36] are listed in Table 2. Among those studies, the data by Balajiva et al. [13] and Winkler and Chipman [14] formed the basis of a broad understanding of the phosphorus equilibria. More careful controlled and detailed studies have since been carried out by Kor et al. [15] and by Suito and his coworkers [16–19]. The

Table 2: Experimental conditions of the literature data on P distribution between slag and metal

Investigators	T,C	Slag, wt%							
		CaO	SiO_2	FetO	MgO	Al_2O_3	MnO	Na_2O	P_2O_5
Balajiva et al. [13]	1585	30~58	8~20	4~38	2~15	<8	<12		4~14
Winkler & Chipman [14]	1500~1700	<42	<41	<80	<30		<30		<20
Kor et al. [15]	1550	31~48	14~33	2~33	6~13				4~13
Suito et al. [16]	1550~1650	<42	<34	11~92	5~29				<1
Suito & Inoue [17]	1550~1650	<34	<33	15~86	6~27				<1
Suito & Inoue [18]	1600	7~28	<27	23~77	5~16				4~5
Suito & Inoue [19]	1550~1650	<35	<31	13~85	6~28		2~5		<4
Ishii & Fruehan [20]	1570~1600	37~46	3~8		4~9	<22			
Shirota et al. [21]	1636~1700	27~52		22~70					2~30
Garlic et al. [22]	1600~1680	27~45	8~24	16~45	8~21		<6		3~5
Nagabayashi et al. [23]	1600	<56	<45	<86	<40				<50
Kunisada & Iwai [24]	1570~1650	10~40	2~40	10~73	4~36			<18	<8
Wrampelmeyer et al. [25]	1550~1700		<12						<1
Usui et al. [26]	1600~1700	26~57	13~35	10~28	<14	<4	3~8		<2
Selin [27]	1593	22~42	15~35	17~31	8~21	<14			<4
Yong et al. [28]	1585~1648	22~52	5~42	2~22	<12	7.2~44	<6		1~12
Schurmann & Fischer [29]	1600,1700	38~58	4~21		2~4	<11			<3
Hino et al. [30]	1550~1650	39~50	20~32	<10		17~30			<5
Banya et al. [31]	1550~1650	30~50				<40			<3
Suito & Inoue [32]	1600	11~31	10~28	20~53	5~18		8~16		
Li et al. [33]	1550~1600	25~42	2~7	30~58	3~13				<3
Lee & Fruehan [34]	1550~1580	33~45	33~40	3~10	13~22				<4
Suito & Inoue [35]	1550	9~30	12~29	28~58	5~11			8~13	<1
Maddocks & Turkdogan [36]	1400,1550	<14	<62	<70	<12	<35	<14	<19	<11

results from the studies by Suito and his coworkers [16–19] show that the measured logarithm of the equilibrium quotient for reaction (11), log(kp) which is defined as equation (12), is a linear function of slag chemistry: (%CaO) + 0.3*(%MgO) – 0.5*(%P_2O_5).

$$2[P] + 5(FeO) = (P_2O_5) + 5Fe \tag{11}$$

$$\log k_p = \log \frac{(wt\%P_2O_5)}{[wt\%P]^2 \cdot (wt\%FetO)^5} \tag{12}$$

The correlation derived by Suito and coworkers [16–19] has been used as a basis to compare the experimental results of steelmaking slag from the various investigators. The comparison of the literature data is shown in Figure 3. It shows that, the experimental results from the independent studies in Figure 3a are consistent with each other, and can be represented by the correlation. However, the experimental results summarized in Figure 3b, show a systematic deviation from the trend line obtained in Figure 3a. Since phosphorus equilibria are strongly dependent on temperature, it is likely that the errors introduced through temperature measurement in the study of Balajava et al. [13], as pointed out by Pathy and Ward [37], could have been responsible for some of the discrepancies as shown in Figure 3b. It also worth to be noted that the reaction time adopted in most of studies summarized in Figure 3a [16, 18, 20, 22, 27, 33] are 3 hours and above, while the reaction time in most of studies in Figure 3b [13, 14, 23, 24] is only 1 hour or less. It is questionable if a short sample holding time of only one hour or less has been sufficient for those studies to reach equilibrium.

4.1 CaO-SiO_2-MgO-FeOn-P_2O_5 system

The CaO-SiO_2-MgO-FeOn-P_2O_5 system is the basic system for slags which occur during steelmaking process, since its components together make up above 90 wt% of the constituents of the steelmaking slags. The data summarized in Figure 3a, which show consistency with each other, was considered to be more reliable and was selected to optimise the model parameters. The overall comparison between the model calculation and experimental measurements on the phosphorus content in the metal equilibrated with the slag is shown in Figures 4. It is evident that there is reasonably good agreement between the model's prediction and experimental measurements over a broad range of concentrations of P in metal within two

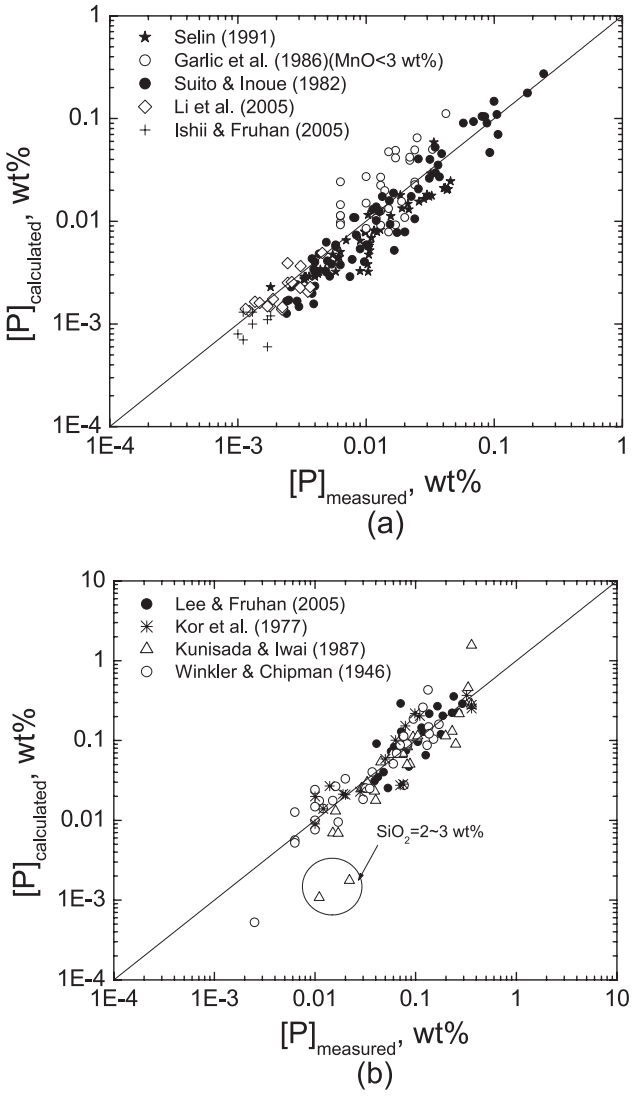

Fig. 4: Comparison of the P solubility in liquid iron calculated by GCA model with the experimental data [14–18, 20, 22, 24, 27, 33, 34].

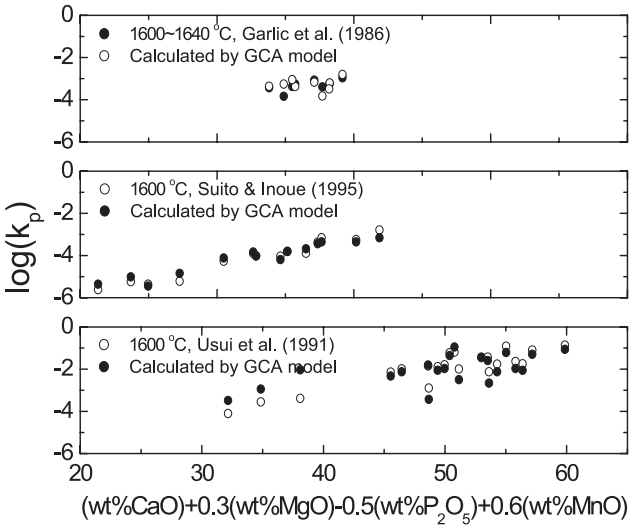

Fig. 5: Comparison of the model calculated $\log(k_p)$ for the MnO containing steelmaking slags with the experimental data [22, 26, 32].

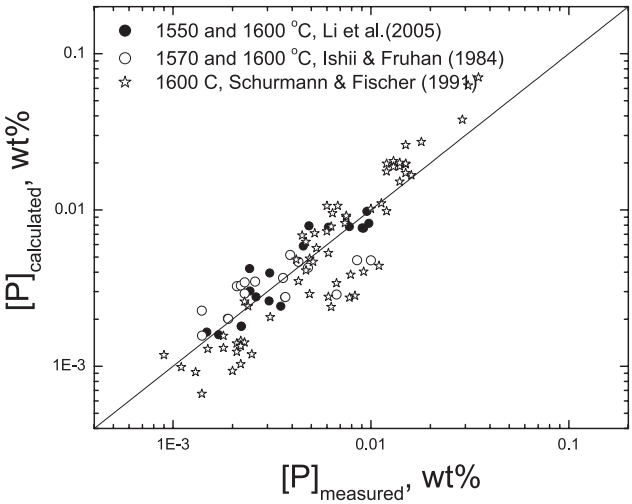

Fig. 6: Comparison of the model calculated P concentration in the liquid iron equilibrated with the Al_2O_3 containing steelmaking slags with the experimental data [20, 29, 33].

orders of magnitude variation. Figure 4b also shows that current model parameters cause relatively large deviation on the P distribution for the slag with low SiO_2 concentration.

4.2 CaO-SiO_2-MgO-FeOn-MnO-P_2O_5 system

The Mn and P distribution between the CaO-SiO_2-MgO-FeOn-MnO-P_2O_5 slag and liquid iron was reported by Garlic et al. [22], Usui et al. [26], and Suito and Inoue [32]. The MnO concentration in the slag varies from 4 to 16 mass%. The MnO-P_2O_5 parameters are obtained by fitting this set of data. The comparison of the model calculation with the experimental data is shown in Figure 5.

4.3 CaO-SiO_2-MgO-FeOn-Al_2O_3-P_2O_5 system

As analysed in the previous section, the P distribution data by Ishii and Fruehan [20], Schurmann and Fischer [29] and Li et al. [33] for the Al_2O_3 free or low Al_2O_3 slag, can be described by the correlations derived by Suito and coworkers [16–19], and was considered to be more reliable. The P_2O_5-Al_2O_3 interaction parameters are optimized against the experimental data by Ishii and Fruehan [20], Schurmann and Fischer [29] and Li et al. [33] with 4 to 22 wt% Al_2O_3 in the slag. The comparison of the calculated P distribution concentrations in liquid iron with the experimental data is shown in Figure 6.

4.4 CaO-SiO_2-MgO-FeOn-Na_2O-P_2O_5 system

The effect of the Na_2O on the P distribution between metal and slag has been investigated by Maddocks et al. [36], Suito and Inoue [35] and Kunisada and Iwai [24]. The equilibrium time adopted in the study by Maddocks et al. [36] is only 20~30 mins. Whether the slag-metal sample can reach equilibrium in such a short time is questionable. Therefore, the P_2O_5-Na_2O parameters are optimized against the experimental data from studies by Suito and Inoue [35] and by Kunisada and Iwai [24]. The comparison of the model calculation and the experimental measurements are shown in Figure 7.

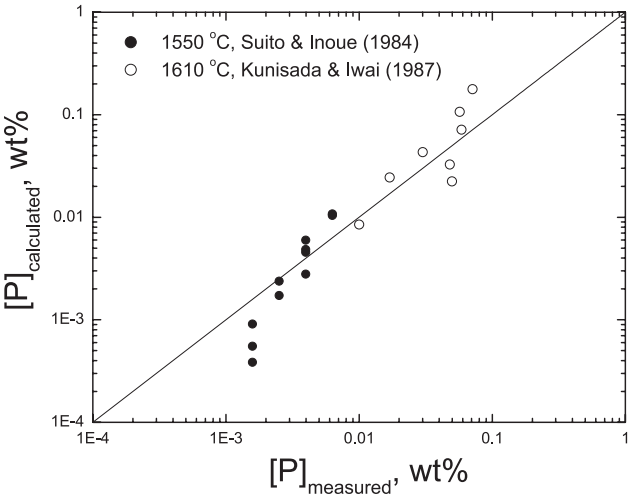

Fig. 7: Comparison of the model calculated P concentration in the liquid iron equilibrated with the Na_2O containing steelmaking slags with the experimental data [24, 35].

5 Modelling of the dephosphorization reactions

The dephosphorization reaction in the BOF can be written as equation (11). The removal of phosphorus to the slag phase depends on the equilibrium constant of reaction (11), which is defined as follows:

$$K_3 = \frac{a_{Fe}^5 \cdot a_{P2O5}}{a_P^2 \cdot a_{FeO}^5} \tag{13}$$

The activity of Fe is very close to unity in this case, and the equation (13) can be rewritten as

$$K_3 = \frac{\gamma_{P2O5} X_{P2O5}}{\gamma_P^2 X_P^2 \cdot a_{FeO}^5} \tag{14}$$

$$\frac{X_{P2O5}}{X_P^2} = K_3 \cdot \gamma_P^2 \cdot \frac{a_{FeO}^5}{\gamma_{P2O5}} \tag{15}$$

Provided that the P activity coefficient in the metal is kept constant, the phosphorus distribution between slag and metal is determined by the activity of FeO and activity coefficient of P_2O_5 in the slag.

The variation of phosphorus distribution between slag and metal with the slag chemistry and the temperature was predicted by using the GCA model. Figure 8 shows that the increase of phosphorus distribution with increasing CaO/SiO_2 in the slag observed in the experiments was reproduced by the calculation. That is simply because there is a strong negative interaction between CaO and P_2O_5. Increase of CaO/SiO_2 ratio leads to the decreasing of the P_2O_5 activity coefficient in the slag, and therefore increases the phosphorus distribution into slag. Both the calculation and the experimental observation showed that the P distribution ratio increased with increasing of Fe_tO content in the slag. After reaching a maximum value, it decreased with further increasing of Fe_tO. This behaviour could be explained by Figure 9. As shown, when the FeO is very low, increasing FeO content would led to a significant increase of FeO activity, and consequently increase the P participation in the slag phase. Further increase of FeO reduces the CaO content in the slag, which increases the γ_{P2O5} in the slag, slow down the increase of $a_{FeO}^5 / \gamma_{P2O5}$, and finally the $a_{FeO}^5 / \gamma_{P2O5}$ reaches a maximum point. After this critical point, increasing Fe_tO would cause the $a_{FeO}^5 / \gamma_{P2O5}$ in the slag to decrease, which in turn resultes in a decreases of the P distribution ratio.

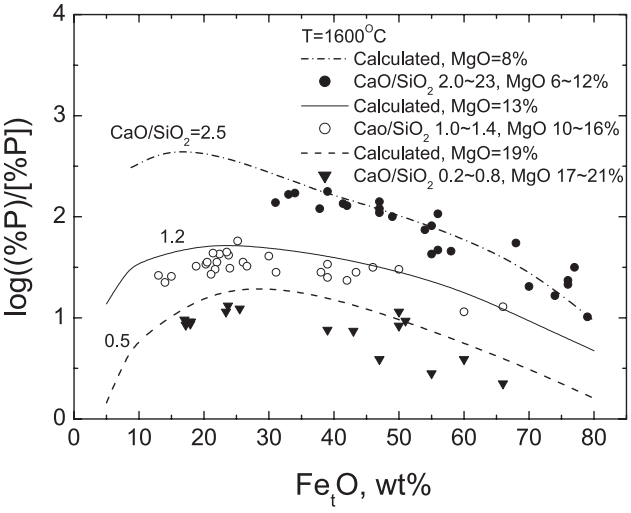

Fig. 8: The effect of FeO and slag basicity on the phosphorus distribution between the CaO-FetO-MgO-SiO_2 slag [16–19] and metal.

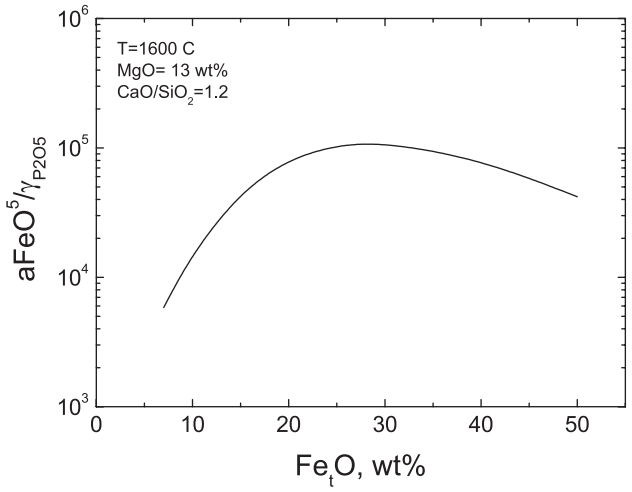

Fig. 9: The effect of FeO content in the slag on the $a_{FeO}^{5} / \gamma_{P2O5}$ ratio in the slag.

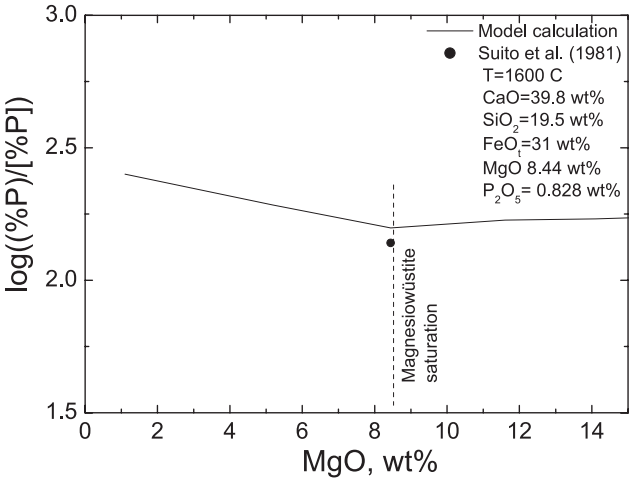

Fig. 11: The effect of MgO content on the phosphorus distribution between the slag and metal.

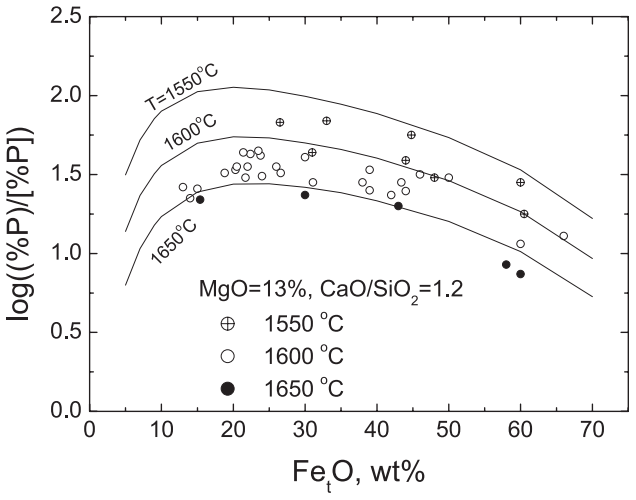

Fig. 10: The effect of FeO and temperature on the phosphorus distribution between the slag and metal. The experimental data are from the studies by Suito and his co-workers [16–19].

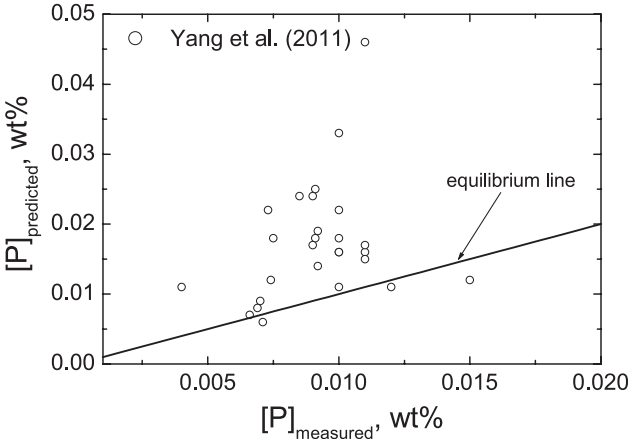

Fig. 12: The comparison of the model calculated and plant measured P content in the metal [38].

Figure 10 showes the effect of temperature on the P distribution between slag and metal. At fixed CaO/SiO_2 and Fe_tO in the slag, the P distribution ratio decreases with increasing temperature. This suggests that lime dephosphorization reaction is exothermic, and is therefore favored at lower temperatures. That is the reason for carrying out dephosphorization under the hot metal conditions such as ladle dephosphorization by some steelmaker.

As shown in Figure 11, the addition of MgO to the slag results in the decrease of the P distribution ratio between slag and metal. That is simply because the lime is the dominant specie in the slag which affects the phosphorus distribution. The addition of MgO, which dilutes the CaO and FeOx concentrations in the slag, leads to lowering of distribution of phosphorus between slag and metal. After reaching the Magnesiowüstite saturation, further addition of MgO decreases the FeO content in the liquid slag by forming the solid solution phase (Magnesiowüstite), which leads increasing the concentration of other components (e.g. CaO) in the liquid slag and tends to increase the phosphorus distribution only slightly according to the calculated results in Figure 11.

Figure 12 shows a comparison of the model calculated and plant measured P content in the metal at the end point of the top-bottom combined blown converter steelmaking process [38]. It can be seen that the P contents in the metal from the equilibrium calculations are systematically lower than that of plant measurements, which indicates that slag and metal are close to but not at the equilibrium yet. Thus kinetics factors that contribute

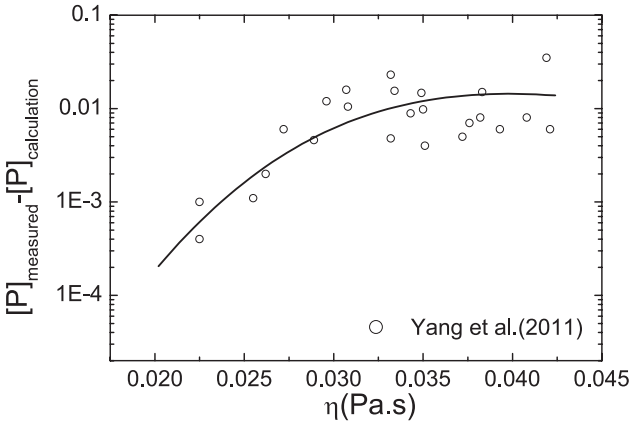

Fig. 13: The correlation of the disequilibrium degree and the slag viscosity.

towards such degree of departure from equilibrium should be considered.

The dephosphorization kinetics in the BOS convertor is dependent on slag properties (e.g viscosity, suspended solid phases in slag, diffusivity,) as well as blowing conditions (hard or soft blown), which effect flux dissolution and slag formation, mixing and emulsification of metal and slag. The degree of dis-equilibrium of phosphorus between metal and slag was studied by Jahanshahi and Belton [39]. They found that there is a marked trend of increasing of disequilibrium degree, defined as $[P]_{Mea.}$-$[P]_{Eql.}$, with increasing solid content in the liquid slag, suggesting that the slag viscosity effects have a major influence. In the present study, the viscosity of the slags from the steelmaking conveter [38] was calculated by using the MPE software [5]. Figure 13 shows that the disequilibrium degree increases with increasing slag viscosities, which agrees with the findings by Jahanshahi and Belton [39]. Minimization of the solid formation in the slag is expected to reduce the disequilibrium degree and improve the phosphorus removal from the metal.

6 Conclusions

The published phase diagrams of some key P_2O_5-containing systems which are relevant to the steelmaking slag and the available experimental data on phosphorus partitioning between liquid iron and slags consisting of SiO_2-Al_2O_3-Fe_2O_3-FeO-MnO-MgO-CaO-Na_2O have been reviewed and assessed. The database of the GCA model has been extended for the system SiO_2-Al_2O_3-Fe_2O_3-FeO-MnO-MgO-CaO-Na_2O-P_2O_5. The developed model database is proved to be able to represent the liquidus temperature of some key P_2O_5-containing systems and the phosphorus distribution ratio between the steelmaking slags and liquid iron reasonable well.

The modelling results show that the phosphorus distribution ratio between the slags and liquid iron reaches a maximum point with increasing FeOx content in the slag. It also shows that the phosphorus distribution to the slag was favored by decreasing the operating temperature and MgO content, and increasing the CaO/SiO_2 ratio in the slag.

Comparison of the phosphorus distribution data from a commercial BOS furnace with model results shows that operating conditions do not permit to reach equilibrium P contents in the metal. The disequilibrium degree of P was found to be increased with increasing slag viscosities. Minimization of the solid formation in the slag is expected to reduce the disequilibrium degree and improve the phosphorus removal from the metal.

Acknowledgement: The authors wish to acknowledge the financial support by CSIRO Process Science & Engineering and ArcelorMittal Maizières, Research and Development. Helpful discussions with Drs S. Jahanshahi and S. Sun of CSIRO are greatly appreciated.

Received: August 8, 2012. Accepted: December 14, 2012.

References

[1] H. Gaye and J. Welfringer, in 2nd International Symposium on Metallurgical Slags and Fluxes, Eds. by Fine, H.A. and Gaskell, D.R., The Metallurgical Society of AIME, Warrendale, 1984, pp. 357–375.
[2] H. Gaye, J. Lehmann, T. Matsumiya and W. Yamada, in 4th International Conference on Molten Slags and Fluxes, The Iron and Steel Institute of Japan, Tokyo, 1992, pp. 103–108.
[3] J. Lehmann and H. Gaye, in 82nd Steelmaking Conference, Chicago, March 21–24, 1999, pp. 463–470.
[4] L. Zhang, S. Jahanshahi, S. Sun, M. Lim, B. Bourke, S. Wright and M. Somerville, Materials Forum, vol. 25 (2001), pp. 136–153.
[5] L. Zhang, S. Jahanshahi, S. Sun, C. Chen, B. Bourke, S. Wright, and M. Somerville, JOM, vol. 54 (2002), pp. 51–56.
[6] J. Lehmann, F. Bonnet and M. Bobadilla, AIST Transactions, vol. 3 (2006), pp. 114–123.
[7] C.H.P. Lupis and J.F. Elliott, Acta Met., vol. 15 (1967), pp. 265–276.
[8] J. Lehmann and L. Zhang, Steel Research Int. 81 (2010) No. 10, pp. 875–879.
[9] Scientific Group Thermodata Europe (SGTE) Substance Database v3, 2008.
[10] Slag atlas, 2nd Edition, (1995), Ed: Verein Deutscher Eisenhuttenleutte, Verlag Stahleisen GmbH, D-Dusseldorf, Germany.

[11] G. Tromel, W. Fix and U. Bongers, Arch Eisenhuttenwes., vol. 40 (1969), pp. 813–819.
[12] G. Tromel, W. Fix and H.E. Wiemer, Arch Eisenhuttenwes., vol. 40 (1969), pp. 673–679.
[13] K. Balajiva, A. Quarrell, and P. Vajragupta, Journal of the Iron and Steel Institute, vol. 153 (1946), pp. 115–145.
[14] T.B. Winkler and J. Chipman, Trans. AIME., vol. 167 (1946), pp. 111–133.
[15] G.J.W. Kor, Met. Trans., vol. 8B (1977), pp. 107–113.
[16] H. Suito, R. Inoue and M. Takeda, Trans. ISIJ, vol. 21 (1981), pp. 250–259.
[17] H. Suito and R. Inoue, Trans. ISIJ, vol. 22 (1982), pp. 869–877.
[18] H. Suito and R. Inoue, Trans. ISIJ, vol. 24 (1984), pp. 40–46.
[19] H. Suito and R. Inoue, Trans. ISIJ, vol. 24 (1984), pp. 257–265.
[20] H. Ishii and R.J. Fruehan, Iron Steelmaker, vol. 24 (1984), pp. 47–54.
[21] Y. Shirota, K. Katohgi, K. Klein, H.-J. Engell and D. Janke, Trans. ISIJ, vol. 25 (1985), pp. 1132–1140.
[22] C. Garlic, S. Jahanshahi and G.R. Belton, unpublished research work (1986), BHP Central Research Laboratories, Shortland, Australia.
[23] R. Nagabayashi, M. Hino and S. Ban-ya, Tetsu-to-Hagane, vol. 74 (1988), pp. 1577–1584.
[24] K. Kunisada and H. Iwai, Trans. ISIJ, vol. 27 (1987), pp. 332–339.
[25] J.C. Wrampelmeyer, S. Dimitrov and D. Janke, Steel Research, vol. 60 (1989), pp. 539–549.
[26] T. Usui, K. Yamada, Y. Kawal, S. Inoue, H. Hiroaki and Y. Nimura, Tetsu-to-Hagane, vol. 77 (1991), pp. 1641–1648.
[27] R. Selin, Scandinavian Journnal of Metallurgy, vol. 20 (1991), pp. 279–299.
[28] R.W. Young, J.A. Duffy, G.J. Hassall and Z. Xu, Ironmaking and Steelmaking, vol. 19 (1992), pp. 201–219.
[29] E. Schurmann and H. Fischer, Steel Research, vol. 62 (1991), pp. 303–313.
[30] M. Hino, S. Yamamoto and S. Banya, Tetsu-to-Hagane, vol. 79 (1993), pp. 27–33.
[31] S. Banya, M. Hino, A. Sato and O. Terayama, Tetsu-to-Hagane, vol. 77 (1991), pp. 361–368.
[32] H. Suito and R. Inoue, Trans. ISIJ, vol. 35 (1995), pp. 266–271.
[33] G. Li, T. Hamano and F. Tsukihashi, ISIJ Int., vol. 45 (2005), pp. 12–18.
[34] C.M. Lee and R.J. Fruhan, Ironmaking and Steelmaking, vol. 32 (2005), pp. 503–508.
[35] H. Suito and R. Inoue, Trans. ISIJ, vol. 24 (1984), pp. 47–53.
[36] W.R. Maddocks and E.T. Turkdogan, Journal of the Iron and Steel Institute, vol. 171 (1952), pp. 128–136.
[37] R.V. Pathy and R.G. Ward, J. Iron and Steel Inst., vol. 188 (1964), pp. 995–1001.
[38] X. Yang, J. Duan, C. Shi, M. Zhang, Y. Zhang and J. Wang, Metall. Mater. Trans. B., vol. 42B (2011), pp. 738–770.
[39] S. Jahanshahi and G.R. Belton, Fifth Int Iron and Steel Congress, Proceedings of the 6th Process Technology Conference, AIME, Washington DC, vol. 6 (1986), pp. 641–659.